Electronic Supplementary Material (ESI) for RSC Advances.

Supporting information

Scalable Synthesis and Surface Stabilization of Li_2MnO_3 NWs for High Rate Cathode Materials in Li-Ion Batteries

Venkat Kalyan Vendra[a,b], Tu Quang Nguyen[a,b] Arjun Kumar Thapa[b], Jacek B. Jasinski[b] , Mahendra K. Sunkara[,a,b]*

[a] Department of Chemical Engineering, University of Louisville, Louisville, KY 40292, USA.
[b] Conn Center for Renewable Energy Research, University of Louisville, Louisville, KY 40292, USA.
* Corresponding author's email: mahendra@louisville.edu

Micron sized MnO_2 powder (Alfa Aesar) and KCl (Sigma Aldrich) and mixed together with water in mortar and pestle to make a paste. A thick layer (~ 100 microns) of this paste is deposited on a stainless steel substrate. The substrate is dried on a hot plate at 70 °C to evaporate the water and is cooled to room temperature and subsequently exposed to an atmospheric plasma flame for 5 minutes. The details of experimental setup of the atmospheric microwave plasma reactor are described elsewhere.[1] An air flow rate of 8 lpm and a plasma power of 750 W were used. The thick film was removed from the substrate while leaving a small part of it on the substrate, to prevent contamination from stainless steel foil. The use of stainless steel foil as the substrate was found to be better than using either quartz or sapphire substrates to make the nanowires. The resulting products on the substrate are then washed with deionized water several times to remove the unreacted salt, and then immersed in 1 M HCl for 2 hours. The remaining products are then heated to 200 °C resulting in manganese oxide.

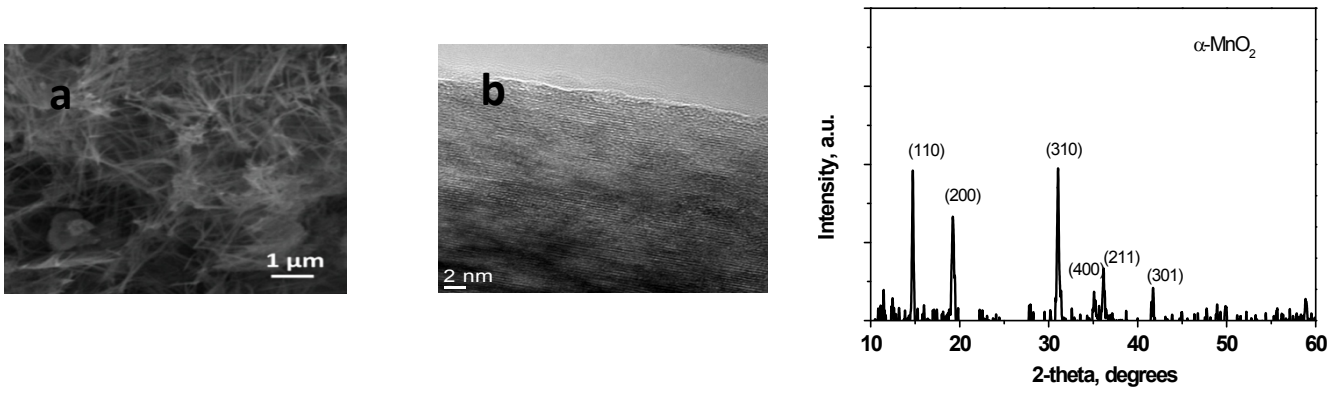

Figure S1(a) Scanning electron microscopy image and (b) high resolution transmission electron microscopy image of manganese oxide NWs synthesized by the solvo plasma process (c) XRD of the MnO_2 NWs synthesized by the solvoplasma process.

Figure S1(a) shows an SEM image of manganese oxide nanowires obtained by the solvo plasma process. The manganese oxide nanowires had an average diameter of about 100 nm and were 4-5 microns in length. High resolution TEM image (Figure S1 (b)) shows that the manganese oxide nanowires are single crystalline. The electrochemical performance of the NW powders with a coin cell configuration. Figure S2 shows the cycling performance of manganese oxide nanowires at 0.2 C rate. A drastic fall in the discharge capacity from 190 mA/g to 50 mAh/g is seen in the first 12 cycles. Figure S2 shows the charge and discharge voltage profiles for first and tenth cycles. In the first discharge cycle in the voltage dropped in a sloping manner until 2.5 V and a plateau was observed, followed by a dropped until a capacity of 100 mAh/g was reached, the voltage then dropped to 1.5 V. The final discharge capacity of 200 mAh/g in the first cycle indicates lithium interaction ratio of 0.64 Li per MnO_2 which is comparable to the reports on manganese oxide for Li ion batteries. However this ratio dropped to 0.16 Li per MnO_2 at the end of the 12 cycle. No plateau regions are observed in the tenth cycle indicating no phase change.

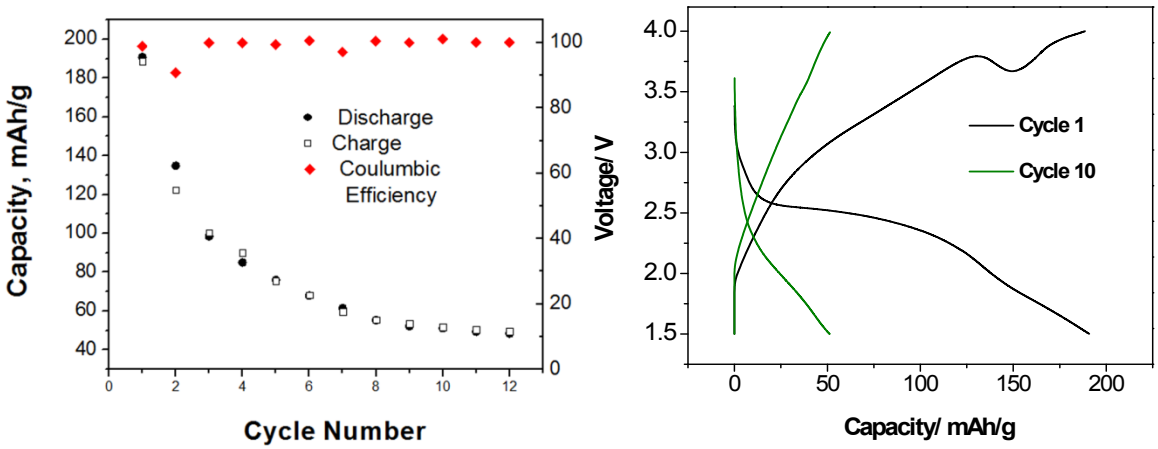

Figure S2. (a) Charge and discharge capacities, columbic efficiency of manganese oxide NWs for the first 12 cycles at 0.2 C rate (b) Charge and Discharge voltage profiles for the cycles 1 and 10.

The MnO_2 NWs retained their morphology after the 12 charge-discharge cycles (Figure S3a) and hence the nanowire pulverization due to volume changes during intercalation and deintercalation cannot explain the loss in capacity. Cyclic voltammetry (Figure S3b) showed that the intercalation and deintercalation were widely separated indicating sluggish intercalation and deintercalation kinetics. The cathodic peak corresponding to Li ion insertion is observed at 2.1 V vs Li/Li^+ while the anodic peak corresponding to Li ion extraction is seen at 3.4 V vs. Li/Li^+.

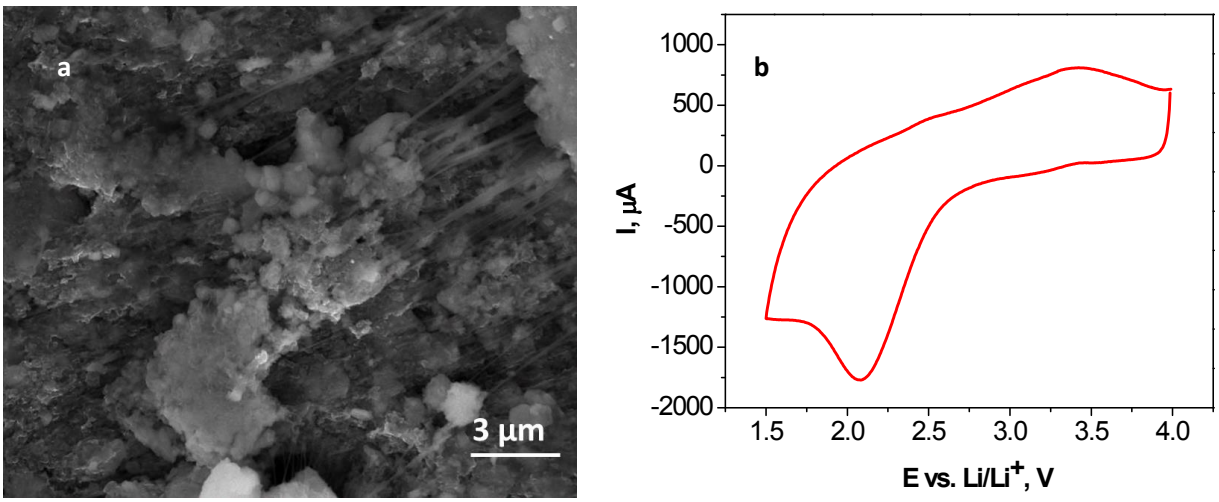

Figure S3. (a) Scanning electron microscopy image shows that the morphology of the MnO_2 NW is still retained after 10 cycles, (b) cyclic voltammogram of the MnO_2 NWs.

The crystal structures of different lithium manganese oxides formed during cycling Li_2MnO_3 are shown in Figure S4. The structures were drawn using Crystal Maker software.

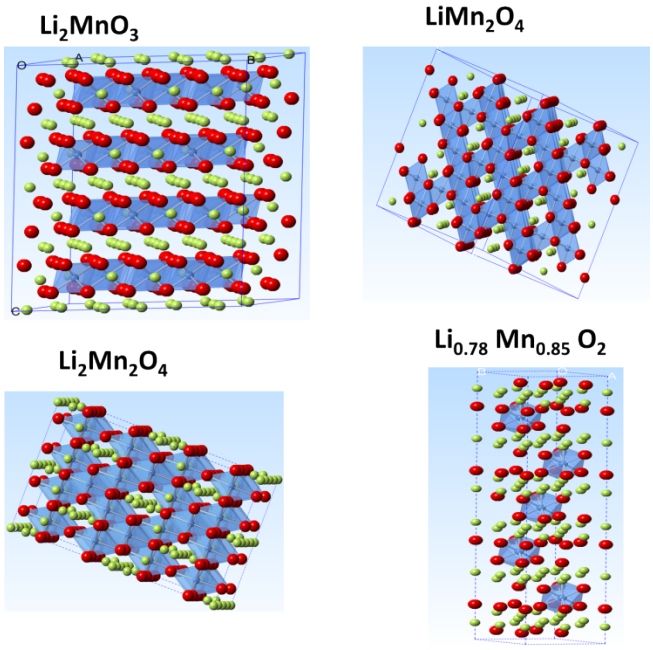

Figure S4. Polyhedra representation of crystal structures of Li_2MnO_3, $Li_2Mn_2O_4$, $Li_2Mn_2O_4$ and $Li_{0.78}Mn_{0.85}O_2$. Lithium atoms are shown in green, managanese atoms in blue and oxygen atoms in red.

The monoclinic Li_2MnO_3 has a layered structure as shown in Figure S4.Cubic $LiMn_2O_4$ spinel structure is formed on the surface of the nanowires during discharge to 3.5 V. Further discharge to 2 V results in the transformation of the cubic spinel to tetragonal $Li_2Mn_2O_4$ and formation of layered $Li_{0.78}Mn_{0.85}O_2$ compound.

Calculation of weight % of Li_2MnO_3 (W1) and $LiMn_2O_4$ (W2)

(a) From HRTEM measurements.

The diameter of the core (D_{core}), and total NW diameter (D_{total}) are measured for the Li_2MnO_3 NWs charged ad discharged to several cycles. and the following formula is compute the weight %.

$$Weight\ \%\ of\ core = \frac{V_{core} * \rho_{core}}{V_{core} * \rho_{core} + V_{shell} * \rho_{shell}}$$

$$= \frac{D_{core}^{2} * \rho_{core}}{D_{core}^{2} * \rho_{core} + (D_{total}^{2} - D_{core}^{2}) * \rho_{shell}}$$

where V is the volume and ρ is the density

In case of a $LiMn_2O_4$ shell and Li_2MnO_3 core nanowire as depicted in Figure 6a, diameter of the core = 31.5 nm ad total NW diameter= 56 nm,

Weight % of Li_2MnO_3 core is calculated as 29.8 % and Weight % of $LiMn_2O_4$ shell is 70.1 %

Similarily for NWs where the core is in the form of $(Li_2O)_x .MnO_2$ (x is very small < 0.12) as shown in Figure 6b (core diameter = 15 nm and total nanowire diamter = 55 nm), weight % of $(Li_2O)_x .MnO_2$ core = 7.4 , weight % of $LiMn_2O_4$ shell is 92.6 %.

(b) From the charge-discharge curves

W1 + W2 = 1

From the charge and discharge profile (Figure 3b), 75 mAh/g can be taken as the intial capacity of Li2MnO3. The first charge-discharge cycle (Figure3b) does not show any plateau region near 4V, and hence LiMn2O4 fraction can be neglected in the first cycle. Based on an earlier report, the capacity of LiMn2O4 at 5 C is 108 mAh/g.[2]

Hence, W1 (75) + W2 (108) = C_{obs}

Where C_{obs} is the observed experimental capacity in Figure 3b.

Based on these two equations the relative weight fraction of Li_2MnO_3 and $LiMn_2O_4$ at different cycles can be calculated and are summarized in the following table.

Table S1. Relative weight fractions of of Li_2MnO3 and $LiMn_2O_4$ at different cycles

Cycle number	Wt % of Li_2MnO_3	Wt % of $LiMn_2O_4$
1	100	0
5	81.1	18.9
10	62.1	37.9
30	43.2	56.8
40	24.2	75.8
100	15.1	84.9

Figure S5 shows the charge-discharge for a Li_2MnO_3 NW sample that is cycled in the 2 V to 4.8 V window on sample that was previously used for C-rate testing in the 2 V to 4.5 V window. (Figure 8). When the sample is charged above 4.5 V, there is significant oxygen evolution and this could lead to formation of non-conformal spinel shell. The pseudo plateau at 4.5 is indicative of oxygen evolution from the electrode. Though high capacity are obtained in this cycling window, a slow capacity fade is observed with increasing number of cycles.

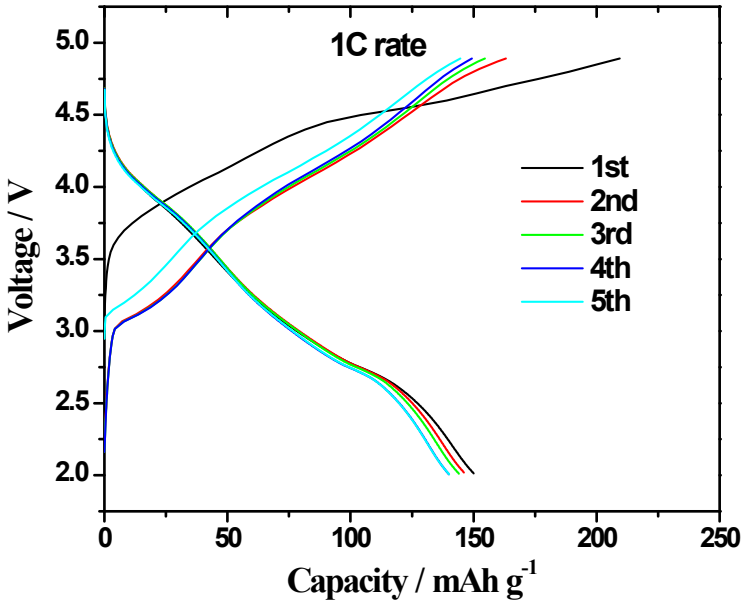

Figure S5. Charge-Discharge curves for Li_2MnO_3 NWs cycled in the 2 to 4.8 V voltage window.

Figure S6 (a) and S6 (b) show the Mn 2p XPS spectra of the samples discharged to 3.5 V and 2 V respectively.

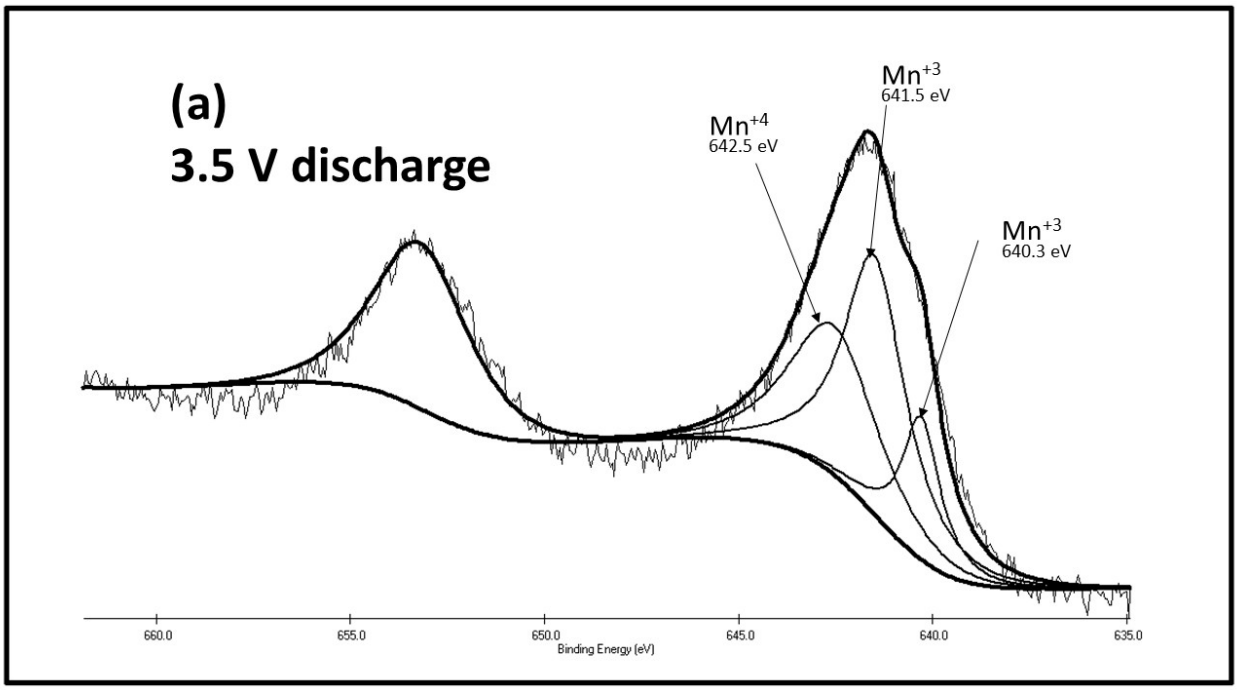

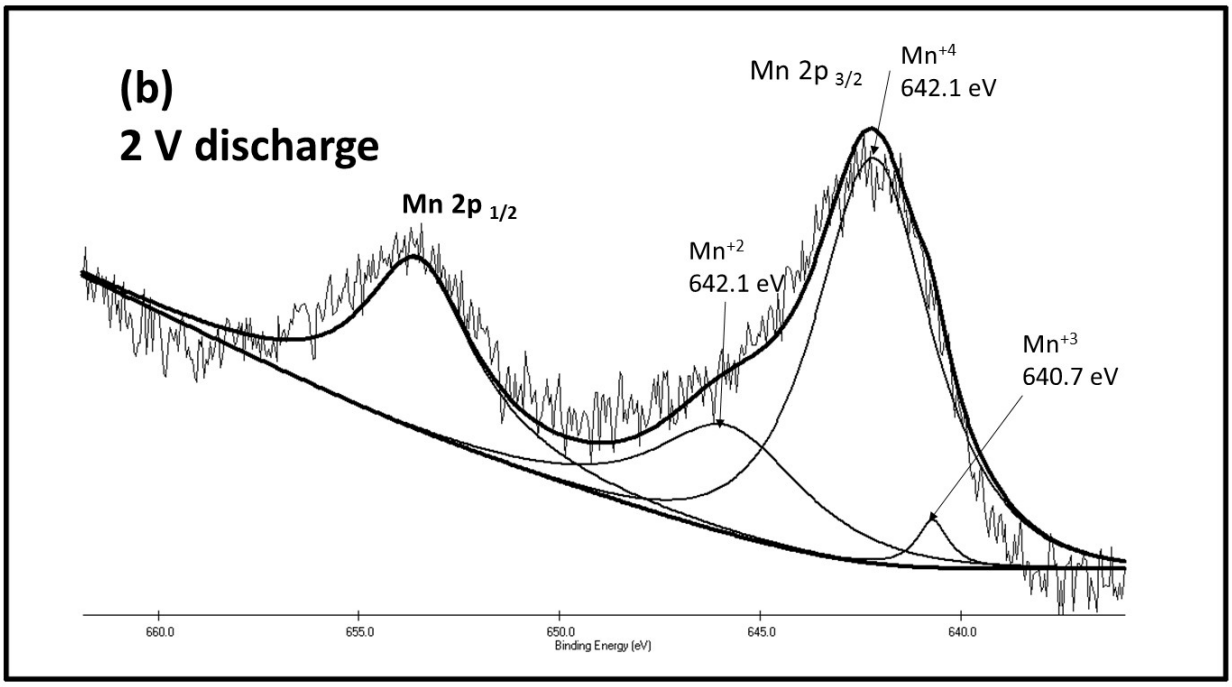

The peak analysis was performed using a XPSPEAK41 software. Analysis of peak positions and comparison with literature[3] shows that in the sample discharged to 3.5 V, Mn is present in +3 and +4 oxidation states and in the sample discharged to 2 V, Mn is present in +3, +4 and +2 oxidation states. The results are in agreement with the phases of lithium manganese oxide observed from the XRD and HRTEM analysis.

References.

1. V. Kumar, J. H. Kim, J. B. Jasinski, E. L. Clark and M. K. Sunkara, *Crystal Growth & Design*, 2011, 11, 2913-2919.
2. H.-W. Lee, P. Muralidharan, R. Ruffo, C. M. Mari, Y. Cui and D. K. Kim, *Nano letters*, 2010, 10, 3852-3856.
3. H. Nesbitt and D. Banerjee, *American Mineralogist*, 1998, 83, 305-315.